Computational study of the response of periodic piezoelectric thin films on substrates

B. Liu,[1] S. Pidugu,[2] and A. Bhattacharyya[1,*]
[1]*Department of Applied Science, University of Arkansas at Little Rock, 2801 South University, ETAS 575, Little Rock, Arkansas 72204-1099, USA*
[2]*Department of Engineering Technology, University of Arkansas at Little Rock, 2801 South University, ETAS 227, Little Rock, Arkansas 72204-1099, USA*
(Received 10 April 2007; revised manuscript received 24 July 2007; published 3 January 2008)

This paper reports a finite element study of periodic, piezoelectric thin film islands on a substrate. The interactions of island radius, interisland periodicity, substrate stiffness, and boundary conditions are examined. It is seen that the degradation of the electromechanical response of the piezoelectric film due to deposition on a substrate is reduced due to two factors: a higher ratio of in-plane area of island to in-plane area of substrate and a lower interisland spacing in the periodic geometry. The effective piezoelectric coefficient of the deposited thin film is different depending on whether the converse or the direct piezoelectric effect is being studied and is larger in the latter case.

DOI: 10.1103/PhysRevB.77.024102 PACS number(s): 77.65.−j, 02.70.Dh, 83.10.Ff, 83.60.−a

I. INTRODUCTION

Deposition of thin ferroelectric films on substrates affects the piezoelectric and ferroelectric properties of the films resulting in an effective film response that is weaker than the response of a freestanding film. This outcome is due to various reasons including clamping effects of the substrate on the film,[1] lattice mismatch,[2] and dislocation generation,[3] all of which are impacted by the geometric dimensions of the film[1,4] as well as the stiffnesses of the film and the substrate.[5]

Equilibrium domain structures in periodic epitaxial thin films were studied by finite element method and compared to experiments for $PbTiO_3$ thin films on MgO substrates.[1] Noting that the domain structures are affected by misfit strain such as due to lattice mismatch, thermal effects, as well as phase transformation, they studied the effects of the lateral dimensions on lattice mismatch. The out-of-plane lattice parameter of the thin film decreased with an increase in the film thickness. Substrate effects need to be factored into a determination of the piezoelectric properties of the thin films based on their effective response after their deposition on the substrate. This was addressed for a lead zirconate titanate (PZT) film on an oxidized wafer[6] and in the determination of piezoelectric coefficients of ferroelectric PZT films with a lead titanate ($PbTiO_3$) or PT bottom electrode between the film and modified Si wafer.[7] Lattice mismatch strains were responsible for an upward shift of the cubic-tetragonal phase transition temperature by about 50 °C in a strontium titanate (STO) film grown on $LaAlO_3$ or LAO single-crystal substrate with $SrRuO_3$ or SRO buffer layers.[8] Lattice mismatch also leads to strain gradients in the thin films which can affect polarization due to flexoelectric coupling; this was studied for various thicknesses of $Ba_{0.5}Sr_{0.5}TiO_3$ or BST thin films with SRO bottom electrodes, deposited on a MgO substrate.[2]

In the context of the piezoelectric response, the effect of the substrate on thin films has been studied quite extensively. In a finite element study of PZT thin films on STO and Si substrates, Li *et al.*[5] demonstrate the degradation in the film piezoelectric properties not only due to the clamping effects of the substrate but also due to substrate bending. While the clamping effects can be compensated by reducing the in-plane dimensions of the film, the bending of the substrate is difficult to avoid, and its magnitude is dependent on the material that is chosen for the substrate. The cumulative effects of the piezoresponse of the thin film are used to determine an effective converse piezoelectric coefficient and compared with the experimentally measured value.[5] Reduction of the in-plane lateral dimensions of the thin film not only mitigates the substrate clamping effects but also serves to relieve internal stresses that may arise out of a lattice mismatch. Since the mismatch is primarily an interfacial phenomenon, a further relief in internal stresses results from increasing the thickness of the thin films. Therefore, tall, slender films are likely to show the least degradation in their electromechanical properties as compared to the properties of freestanding films.

In order to get an electromechanical response over a large area, patterning the film into periodic structures on the substrate is the method of choice. This is especially relevant when device miniaturization is the issue at hand.[9] There is also evidence that patterning contributes to a significant improvement in the effective properties of an epitaxial PZT thin film on a STO substrate.[9] The 100 nm PZT thin films with a square cross section (lateral dimensions of 300 nm and less) were patterned on STO in a square-periodic array. While the enhancement in the property was attributed to the vanishing of *a* domains, the effect of the deformation field in the film and the substrate due to the geometric periodicity of the PZT islands cannot be completely ruled out.

In this paper, we study the effect of electromechanical boundary conditions on the response of periodic thin film islands on a thick substrate. For the purpose of numerical computation, we choose zinc oxide (ZnO) and strontium titanate ($SrTiO_3$) or STO for the thin film and substrate, respectively. The bulk of the work focuses on islands with circular cross section. However, results are also compared to that of islands with square cross section (but having the same cross-sectional area as the circular shape). The interactions of island geometry (thickness and radius) with elastic prop-

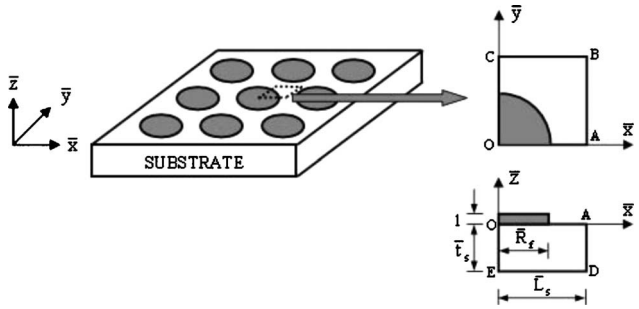

FIG. 1. Schematic diagram of a $\bar{x}\bar{y}$-periodic structure with circular thin film islands and geometric details of a quarter unit cell.

erties of the substrate, interisland spacing, and electromechanical boundary conditions (free, x periodic, and xy periodic) are studied. The predominant effect of the periodicity is on the clamping effects of the substrate. Both responses—the converse as well as the direct piezoelectric effects—are addressed. These responses are also a measure of the effective piezoelectric compliance coefficient d_{zzz}. While d_{zzz} for a freestanding film is identical regardless of whether the converse or the direct effect is studied (as d_{zzz} is a material property), such an identity is not guaranteed for the effective d_{zzz} when the thin film is attached to a substrate.

The scientific notation used in the text is summarized here. Vectors will be represented using an upper case Latin letter with an overhead arrow, e.g., $\vec{D}$. A second order tensor will be represented with a boldface, lower case Greek letter, $\boldsymbol{\sigma}$, a third order tensor with a boldface lower case Latin letter, $\mathbf{d}$, and a fourth order tensor with a boldface upper case Latin letter, $\mathbf{M}$. Components of vectors and second/third/fourth order tensors will be denoted with the corresponding letters in regular type and with one and two/three/four subscripts, respectively. Thus, the component of the elastic compliance tensor $\mathbf{M}$ relating the x-axis component of the strain to the x-axis component of the stress is written as M_{xxxx}.

II. PERIODIC THIN FILMS ON A SUBSTRATE

A. Constitutive equations, nondimensionalization, and boundary conditions

The electromechanical constitutive equations of the piezoelectric thin film are[10]

$$\boldsymbol{\varepsilon} = \mathbf{M}\boldsymbol{\sigma} + \mathbf{d}^T\vec{E}, \quad \vec{D} = \mathbf{d}\boldsymbol{\sigma} + \boldsymbol{\kappa}^{\sigma}\vec{E}, \tag{1}$$

where $\boldsymbol{\varepsilon}$ is the strain tenser, $\mathbf{M}$ is the elastic compliance tensor, $\boldsymbol{\sigma}$ is the stress tensor, $\mathbf{d}$ is the third order piezoelectric compliance tensor (where T indicates transpose), $\vec{E}$ is the electrical field vector, $\vec{D}$ is the dielectric displacement vector, and $\boldsymbol{\kappa}^{\sigma}$ is the tensor of dielectric constants at constant stress. The substrate is taken to be purely elastic and its constitutive equation will be given by $\boldsymbol{\varepsilon}=\mathbf{M}\boldsymbol{\sigma}$. Note that in the second equation of Eqs. (1), $\vec{E}=-\vec{\nabla}\varphi$, where φ is the electric potential.

The geometry of the boundary value problem is shown in Fig. 1. It is a square-periodic structure of circular islands of thin films on the xy plane. In our parametric studies, we have also compared the results for the circular islands with a periodic array of rectangular films of identical thickness and identical cross-sectional area on the xy plane. The entire study is carried out using nondimensional parameters; these are indicated with a "bar" over their dimensional counterparts. Thus,

$$\bar{x} = \frac{x}{t_f}, \quad \bar{y} = \frac{y}{t_f}, \quad \bar{z} = \frac{z}{t_f}, \quad \bar{\mathbf{M}} = M_{xxxx}^{-1}\mathbf{M}, \quad \bar{\mathbf{d}} = d_{zzz}^{-1}\mathbf{d}, \tag{2}$$

where x, y, and z are the spatial coordinates, t_f is the thickness of the film, M_{xxxx} is the component of the compliance tensor relating the x-axis component of the strain to the x-axis component of the stress, and d_{zzz} is the component relating the z component of the electric displacement to the z-axis component of the stress. With Eqs. (2), Eqs. (1) are nondimensionalized as

$$\boldsymbol{\varepsilon} = \bar{\mathbf{M}}\bar{\boldsymbol{\sigma}} + \bar{\mathbf{d}}^T\bar{\vec{E}}, \quad \bar{\vec{D}} = \bar{\mathbf{d}}\bar{\boldsymbol{\sigma}} + \bar{\boldsymbol{\kappa}}^{\sigma}\bar{\vec{E}}, \tag{3}$$

where the following nondimensional parameters have been identified:

$$\bar{\boldsymbol{\sigma}} = \boldsymbol{\sigma}M_{xxxx}, \quad \bar{\vec{E}} = \vec{E}d_{zzz}, \quad \bar{\vec{D}} = \vec{D}\frac{M_{xxxx}}{d_{zzz}}, \quad \bar{\boldsymbol{\kappa}}^{\sigma} = \boldsymbol{\kappa}^{\sigma}\frac{M_{xxxx}}{d_{zzz}^2}. \tag{4}$$

Because of symmetry, only a quarter of the model needs to be analyzed (see Fig. 1). The displacements of a material point along x, y, and z are denoted as u_x, u_y, and u_z, respectively; these are the orthogonal components of the displacement vector $\vec{u}$. The parametric studies primarily focus on two types of electromechanical boundary conditions: periodic and free. The periodic boundary conditions[11] are stated below. Items (i)–(viii) are the mechanical boundary conditions, whereas (ix) and (x) are the electrical boundary conditions.

(i) Surface $OC(\bar{x}=0):\bar{u}_x=0$, where $\bar{u}_x$ indicates the component of the displacement vector along the $\bar{x}$ axis.

(ii) Surface $AB(\bar{x}=\bar{L}_s):\bar{u}_x=\bar{u}_x(\bar{L}_s,0,0)$.

(iii) Surface $OA(\bar{y}=0):\bar{u}_y=0$.

(iv) Surface $CB(\bar{y}=\bar{L}_s):\bar{u}_y=\bar{u}_y(0,\bar{L}_s,0)$.

(v) Surface $ED(\bar{z}=-\bar{t}_s):\bar{u}_z=0$. This boundary condition simulates the experimental condition of a rigid platform on which the substrate has been placed.

(vi) At $E(\bar{x}=0,\bar{y}=0,\bar{z}=-\bar{t}_s):\bar{\vec{u}}=0$.

(vii) Interface between film and substrate $(\bar{z}=0):[[\bar{\vec{u}}]]=0$, $[[\bar{\boldsymbol{\sigma}}\hat{n}]]=0$, where $[[\ ]]$ indicates jump across the interface of a given quantity and $\hat{n}$ is a unit normal to a surface and directed outward from the volume that is enveloped by the surface.

(viii) On film surface $(\bar{z}=1):\bar{\boldsymbol{\sigma}}\hat{n}=\bar{F}_z/\bar{A}$. Here, $\bar{F}_z=F_z(M_{xxxx}/t_f^2)$, where F_z is the normal mechanical load applied on the thin film, and $\bar{A}=\pi\bar{R}_f^2$.

(ix) On film interface $(\bar{z}=0):\bar{\varphi}=0$, where $\bar{\varphi}=(d_{zzz}/t_f)\varphi$.

(x) On film surface $(\bar{z}=1):\bar{\varphi}=-\bar{E}_z$, where $\bar{E}_z$ is the normalized external electric field across the film thickness.

TABLE I. The material properties of the ZnO film (Ref. 12).

Material property	Value (GPa)	Material property	Value (C/m^2)
M_{xxxx}	209	e_{xxz}, e_{yyz}	−0.48
M_{xxyy}	120.5	e_{zxx}, e_{zyy}	−0.573
M_{xxzz}, M_{yyzz}	104.6	e_{zzz}	1.321
M_{zzzz}	210.6		
M_{xzxz}, M_{yzyz}	42.3		
M_{xyxy}	44.25		

Computations with the free boundary conditions are modeled by replacing conditions (i) and (iv) above with a traction-free condition, $\bar{\boldsymbol{\sigma}}\hat{n}=0$. The converse piezoelectric effect is modeled by setting $\bar{F}_z=0$ in (viii) above, whereas the direct piezoelectric effect is modeled by setting $\bar{E}_z=0$ in (x).

The calculations are based on the material properties of a zinc oxide (ZnO) thin film[12] and a strontium titanate ($SrTiO_3$) or a STO substrate.[13] The former is transversely isotropic, and in the calculations, we assume that the axis of transverse isotropy is perpendicular to the plane of the substrate. The properties of ZnO are listed in Table I.

The STO substrate is taken to be elastically isotropic; its Young's modulus and the Poisson's ratio are taken as $Y=189.7$ GPa and $\nu=0.232$, respectively.[13] We define a relative stiffness ratio γ due to biaxial loading on film to that of the substrate as $\gamma=[Y(M_{xxxx}+M_{xxyy})/(1-\nu)]$. For the assumed material properties, the material stiffness ratio works out to $\gamma=3.2317$; unless otherwise stated, the above mentioned material properties are used in the computations. The converse piezoelectric effect is computed by setting $E_z=5$ V/m, whereas the direct effect is computed by setting $F_z/A=10.45\times10^9$ N/m^2. While ZnO is piezoelectric, the theory outlined in this paper can be used to model the initial electroelastic response to an external electric or mechanical field of a piezoelectric film that is also ferroelectric. In that case, the incremental electromechanical response of the film during external loading and prior to phase transformation may be accounted for by replacing $\boldsymbol{\varepsilon}$, $\vec{D}$ and $\boldsymbol{\sigma}$ [in Eq. (1)] with their incremental counterparts, respectively. Further, the material properties—**M**, **D**, and $\mathbf{k}^{\sigma}$—will take their position dependent values depending on the variant orientation in the microstructure of the deposited film.

III. PARAMETRIC STUDIES

A. Optimization of the finite element model

The software ABAQUS is used for the finite element computations. Three dimensional solid elements (type C3D6E) with optimized grid seeds are employed to mesh the model; an example is shown in Fig. 2. The mesh used in the film is taken to be uniform on the xy plane and nonuniform along the z direction. The nonuniformity is defined by the bias ratio G_1/G_N, where G_1 and G_N indicate the length of the first and the Nth elements along the z direction for the first and the Nth elements and the number of elements along the z direction (defined by N). The user is required to provide the value of the bias ratio and N; the software generates all N elements. An identical nonuniformity in mesh generation is implemented in the substrate from the interface to a depth equal to the thickness of the film. Below this depth, a uniform mesh is taken (with a total of 20 elements in the current calculations). The number of elements along the x direction is taken as M. Figure 3 is a plot of the normalized vertical displacement of the center of the top surface of the film relative to an identical freestanding film subjected to an electric field along the z direction (referred henceforth as "relative normalized displacement") with respect to the bias ratio for different values of N. These results have all been computed at $\bar{R}_f$, $\bar{L}_s$, and M equal to 10, 100, and 10, respectively. The displacements are not very sensitive for values of $N=10$ and higher and for bias ratios of 10 and higher. We have chosen $N=20$ and a bias ratio of 10, and then repeated these calculations for values of M at 5, 10, 15, 20, and 25; the relative normalized displacements are 0.1306, 0.2213, 0.2159, 0.2172, and 0.2169, respectively. Thus, for the parametric studies, we have taken $N=20$, bias ratio=10, and $M=20$.

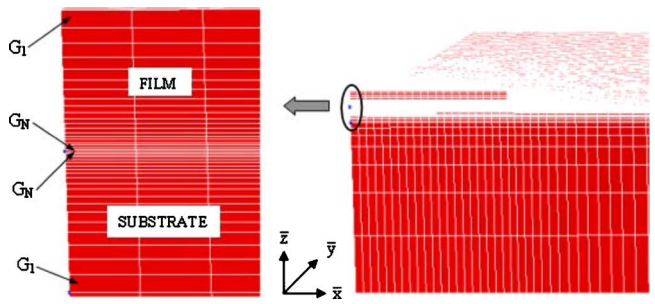

FIG. 2. (Color online) Finite elements mesh with bias ratio (bias ratio=G_1/G_N).

B. Results

Figure 4 is a study of the relative normalized displacement for a fixed normalized radius $\bar{R}_f=5$ of a circular thin

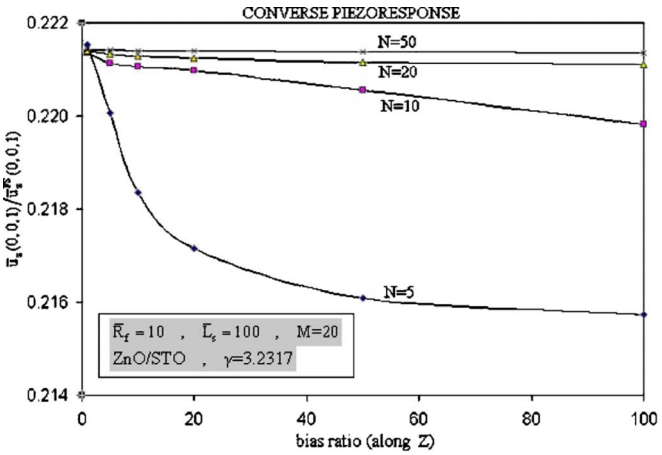

FIG. 3. (Color online) Effect of bias ratio and number of elements along film thickness on the relative normalized displacement when an electric field is applied normal to the surface of the film (the converse piezoelectric effect).

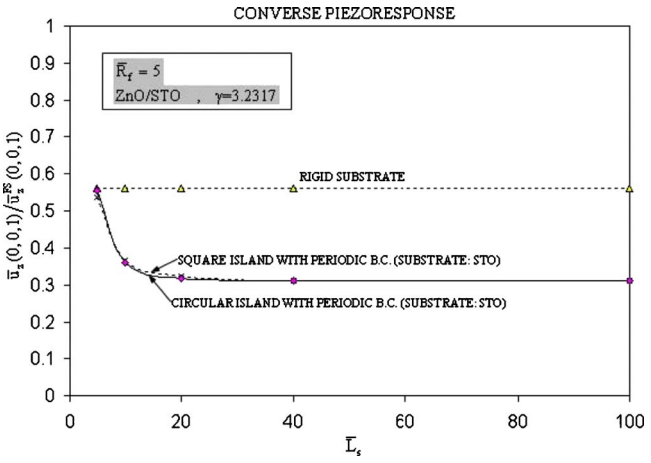

FIG. 4. (Color online) The dependence of relative normalized displacement on interisland spacing for soft substrates under $\bar{x}\bar{y}$-periodic boundary conditions and rigid substrates when an electric field is applied normal to the surface of the film (the converse piezoelectric effect).

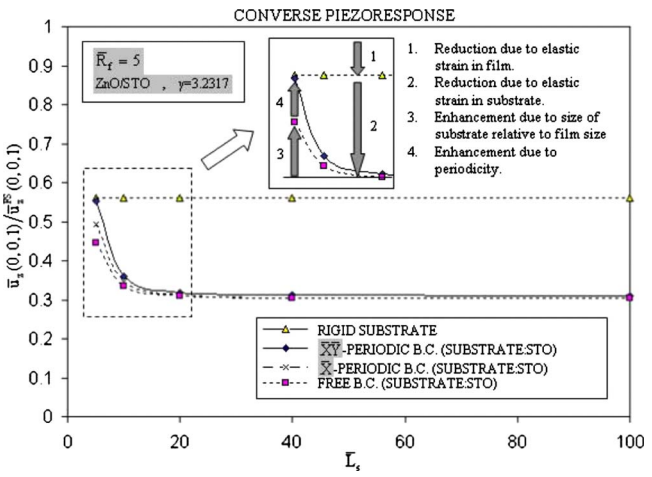

FIG. 5. (Color online) The dependence of relative normalized displacement on interisland spacing for soft substrates under $\bar{x}$-periodic, $\bar{x}\bar{y}$-periodic, and free boundary conditions and rigid substrates (the converse piezoelectric effect).

film with respect to an increase in $\bar{L}_s$; this latter quantity is half of the spacing between the centers of neighboring thin film islands (along the x or the y axis). The effect of the substrate is to diminish the displacement corresponding to the converse piezoelectric strain; all values of the relative normalized displacement are less than unity. The soft substrate with circular islands (the lowest curve) causes a larger reduction compared to the rigid substrate. Notice that at values of $\bar{L}_s=20$ and higher, the relative normalized displacement is insensitive to different values of $\bar{L}_s$. Thus, over this range, the interisland interaction is negligible and may as well be simulated by considering each unit of the periodic cell as an independent domain subjected to free boundary conditions; we have confirmed this result with our computations. The film responses in this range (where interisland interactions are negligible) were studied by Li *et al.*[5] Below $\bar{L}_s=20$, the relative normalized displacement increases sharply, and specifically, this contribution comes from the reduced elastic deformation of the substrate. This can be expected since a reduced interisland distance results in an increased cell-to-cell interaction and a resulting decrease in bending of the substrate out-of-plane and Poisson contraction in-plane. Also included in this figure are the results of computations for thin film islands with a square cross section, where the areas of the square and circular films are taken identical for comparison. Notice that both geometries give a very similar response, with the circular shape giving a slightly better response when $\bar{R}_f \sim \bar{L}_s$.

To study the effect of periodicity, we have given the relative normalized displacement with respect to $\bar{L}_s$ in Fig. 5 for three types of boundary conditions: free, $\bar{x}$ periodic, and $\bar{x}\bar{y}$ periodic. The difference between these boundary conditions appears below $\bar{L}_s=20$. The effect of the periodicity primarily restricts the Poisson contraction in plane of the substrate and reduces the bending of the substrate out of plane. As expected, the effect is the greatest for the xy-periodic boundary condition and the least for the free boundary condition. With respect to the converse piezoelectric strain of the freestanding film, the overall response of the deposited thin film is different due to four reasons [indicated by the numbers (1)–(4) in Fig. 5]: (1) elastic strain of the film when attached to the substrate, (2) elastic strain due to deformation of the substrate, (3) elastic strain due to increasing in-plane area of thin film island relative to in-plane area of substrate (inferred from the fact that this case corresponds to "free" boundary conditions), (4) elastic strain due to periodicity of the islands. Items (1) and (2), which lead to a degradation of the electromechanical response of the deposited thin film compared to its freestanding counterpart, were identified by Li *et al.*[5] in their paper. Items (3) and (4) are responsible for *a reduction* in the degradation of the electromechanical response. This is also demonstrated by a comparison of the contour plots of the vertical displacement $\bar{u}_z$ for the three types of boundary conditions in Fig. 6; notice that the substrate with the free boundary condition has the largest volume (the "yellow" region or the middle white region when viewed in grayscale) with the largest contractions along the z direction.

Figure 7 uncovers the effect of the periodic boundary condition vis-à-vis the stiffness of the substrate in somewhat more detail for $\bar{R}_f=5$ and $\bar{L}_s=5$. This corresponds to the case when each circular thin film island is in point contact with its

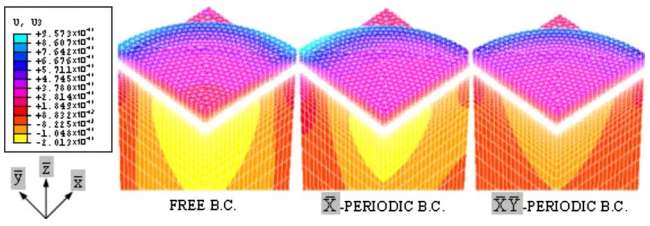

FIG. 6. (Color online) Comparison of displacement along the z axis, $\bar{u}_z$, for free boundary condition, $\bar{x}$-periodic boundary condition, and $\bar{x}\bar{y}$-periodic boundary condition.

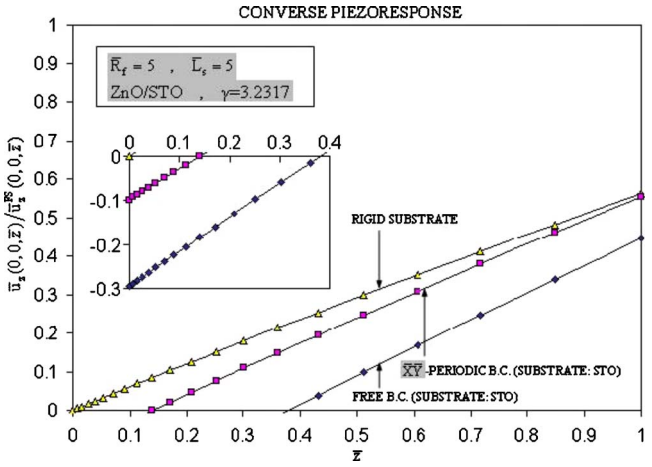

FIG. 7. (Color online) The dependence of the relative normalized displacement with respect to depth along thin film for soft substrates under periodic and free boundary conditions and rigid substrates when an electric field is applied normal to the surface of the film (the converse piezoelectric effect).

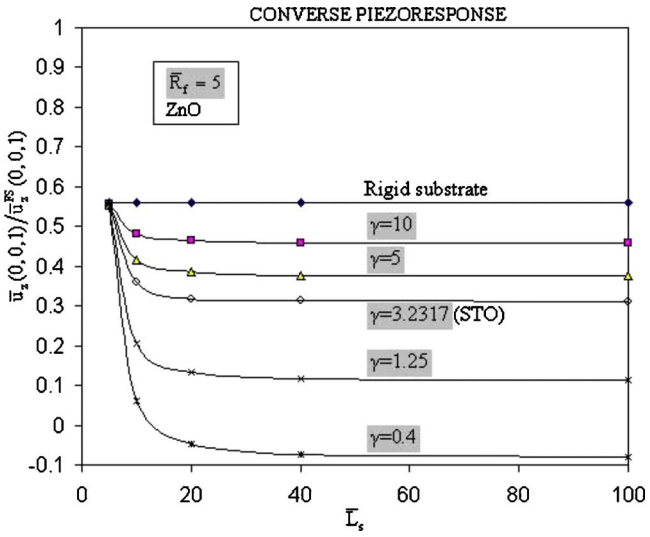

FIG. 8. (Color online) The dependence of the relative normalized displacement with respect to the relative stiffness ratio γ. All calculations in this figure are subjected to $\bar{x}\bar{y}$-periodic boundary conditions. The reported data correspond to an electric field that is applied normal to the surface of the film (the converse piezoelectric effect).

neighbor. The relative normalized displacement is shown as a function of height ($\bar{z}$ coordinate) from the interface and along the thickness of the thin film. Negative displacements at $\bar{z}=0$ indicate that the interface bends toward the interior of the substrate. The magnitude of the displacement corresponding to the soft substrate subjected to free boundary conditions is significantly higher than the displacement corresponding to the soft substrate subjected to the periodic boundary conditions. In fact, for the chosen material properties, the effect of the boundary condition on the deformation of the substrate is much higher than the stiffness effect of the substrate. This contrast is maintained as $\bar{z}$ increases, with a slightly higher rate of increase for the soft substrate with free boundary conditions than the other cases (i.e., the slope of the lowest curve is somewhat higher than the other two). The effect of the relative stiffness ratio is studied in Fig. 8 for $\bar{R}_f=5$ and different values of $\bar{L}_s$. A comparatively stiffer substrate (high value of γ) results in a higher displacement; if the substrate is much softer than the film, $\gamma=0.4$, the relative displacement becomes negative, which was identified by Li *et al.*[5] in their paper.

The relative normalized displacement is studied in Fig. 9 at various values of the normalized radius and interisland spacing. Notice that at any given value of the interisland spacing, there is a nonmonotonic dependence of the relative normalized displacement on the relative radius; this is shown in the inset for $\bar{L}_s=100$. This can be anticipated. As $\bar{R}_f$ decreases toward zero, it steadily becomes decoupled from the clamping effect of the substrate and in the limit $\bar{R}_f \to 0$, the stress field becomes truly one dimensional (along the z direction) and the relative normalized displacement approaches 1. On the other hand, as $\bar{R}_f$ increases, the clamping effect of the substrate increases to the extent that the in-plane strain field in the film can be taken to vanish, i.e., $\varepsilon_{xx}=0$ and $\varepsilon_{yy}=0$. For this approximation, the relative normalized displacement turns out to be $\bar{u}_z/\bar{u}_z^{FS}=\{1-[2M_{xxzz}/(M_{xxxx}+M_{xxyy})]\bar{d}_{zxx}\}$, where superscript FS indicates the freestanding film; the numerical value of this ratio turns out to be 0.5441 (for the material properties cited in this paper). It is between the values of 1 and 0.5441 that the relative normalized displacement changes nonmonotonically with $\bar{R}_f$. Notice from Fig. 9 (and not its inset) that at lower values of $\bar{R}_f$, the relative normalized displacement corresponding to $\bar{R}_f=\bar{L}_s$

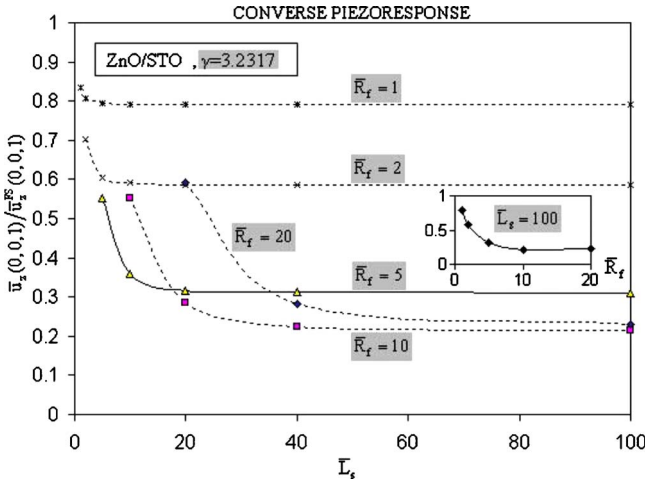

FIG. 9. (Color online) The dependence of the relative normalized displacement with respect to interisland spacing for different values of the radius of each island. The inset is the relative normalized displacement with respect to island radius at a given value of interisland spacing. All calculations in this figure are for a soft substrate subjected to periodic boundary conditions. The reported data correspond to an electric field that is applied normal to the surface of the film (the converse piezoelectric effect).

(i.e., the left end of each curve) increases. This increase corresponds to the situation where smaller islands are deposited in a dense packing arrangement and is due to reasons (3) and (4) discussed in Fig. 5. These reasons could have contributed, in part, to a sharp increase in the piezoelectric response of ferroelectric epitaxial PZT thin films on a STO substrate[9] (we draw this conclusion in spite of the fact that the specific results in this paper pertain to ZnO films on STO substrate).

For the freestanding film, the piezoelectric coefficient d_{zzz} connects the electric field E_z (all other components of the electric field being zero) to the deformation u_z during the converse effect through $d_{zzz}=u_z(0,0,z)/(t_f E_z)$, whereas it connects the stress component σ_{zz} at the top surface of the film (all other components of the stress being zero) to the electric displacement D_z during the direct piezoelectric effect through $d_{zzz}=D_z(0,0,1)/\sigma_{zz}$. However, when the film is attached to a substrate, the normalized "effective" piezoelectric coefficient that will govern the converse effect and the direct effect may be estimated using the relations $\bar{d}_{zzz}^{\text{effective}}=\bar{u}_z(0,0,1)/\bar{E}_z$ and $\bar{d}_{zzz}^{\text{effective}}=\bar{D}_z(0,0,1)/\bar{\sigma}_{zz}$, respectively. These are not guaranteed to be identical. In that context, it would be interesting to see the difference under the two different boundary conditions. The normalized effective piezoelectric coefficient is shown in Fig. 10 at various values of $\bar{R}_f$ and at two different values of $\bar{L}_s$ for both the converse effect (solid lines) and the direct effect (dashed lines). It is seen that when $\bar{R}_f<5$ (and is substantially lower than both values of $\bar{L}_s$), the effective piezoelectric coefficient is practically identical for the converse and direct response while being somewhat degraded from that of the freestanding film. Beyond $\bar{R}_f>5$, the effective coefficient is, in general, different and is higher during the direct effect as compared to the converse effect.

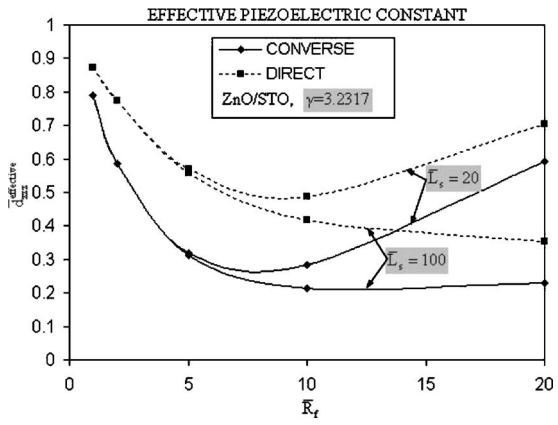

FIG. 10. The dependence of the effective normalized piezoelectric coefficient corresponding to the converse and direct effects with respect to island radius for given values of interisland spacing. All calculations in this figure are for a soft substrate subjected to periodic boundary conditions.

IV. CONCLUSIONS

A finite element study of a square-periodic array of thin film piezoelectric islands was implemented. The entire study is carried out using nondimensional parameters. A lower periodicity and a higher ratio of the island radius with respect to the in-plane dimension of the periodic unit cell are instrumental *in reducing* the degradation in the electromechanical response of the thin film attached to the substrate. A nonmonotonic response with respect to the radius of the film and a tendency of the deposited film to approach a free or a clamped state for either a very small or very large radius, respectively, are also discussed and explained. The effective piezoelectric coefficients calculated from the converse and direct effects are generally lower than the bulk value; this degradation is not as much during the direct effect as it is during the converse effect.

ACKNOWLEDGMENTS

Financial support from the National Science Foundation (NSF)-EPSCOR program is acknowledged (Award No. EPS-0236967 to University of Arkansas at Fayetteville and Subcontract No. SA0402138 from University of Arkansas at Fayetteville to University of Arkansas at Little Rock).

*FAX: 501-569-8020; axbhattachar@ualr.edu; URL: http://mems.appsci.ualr.edu

[1] K. Lee, H. Yi, W. Park, Y. K. Kim, and S. Baik, J. Appl. Phys. **100**, 051615 (2006).
[2] G. Catalan, B. Noheda, J. McAneney, L. J. Sinnamon, and J. M. Gregg, Phys. Rev. B **72**, 020102 (2005).
[3] S. P. Alpay, I. B. Misirlioglu, V. Nagarajan, and R. Ramesh, Appl. Phys. Lett. **85**, 2044 (2004).
[4] C. Lichtensteiger, J. M. Triscone, J. Junquera, and P. Ghosez, Phys. Rev. Lett. **94**, 047603 (2005).
[5] J. Li, L. Chen, V. Nagarajan, R. Ramesh, and A. L. Roytburd, Appl. Phys. Lett. **84**, 2626 (2004).
[6] C. L. Canedy, H. Li, S. P. Alpay, L. Salamanca-Riba, A. L. Roytburd, and R. Ramesh, Appl. Phys. Lett. **77**, 1695 (2000).
[7] K. Lefki and G. J. M. Dormans, J. Appl. Phys. **76**, 1764 (1994).
[8] F. He, B. O. Wells, S. M. Shapiro, M. von Zimmermann, A. Clark, and X. X. Xi, Appl. Phys. Lett. **83**, 123 (2003).
[9] S. Buhlmann, B. Dwir, J. Baborowski, and P. Muralt, Appl. Phys. Lett. **80**, 3195 (2002).
[10] W. G. Cady, *Piezoelectricity: An Introduction to the Theory and Applications of Electromechanical Phenomena in Crystals* (Dover, New York, 1964).
[11] Z. Bo, Ph.D. thesis, Texas A&M University, 1996.
[12] G. Carlotti, G. Socino, A. Petri, and E. Verona, Ultrasonics Symposium Proceedings, 1987 (unpublished), p. 295.
[13] H. Ledbetter, M. Lei, and S. Kim, Phase Transitions **23**, 61 (1990).